

# Mechanical behaviour of pitting corrosion of flexural and shear reinforcement and its effect on structural reliability of corroding RC beams

Mark G. Stewart \*

*Centre for Infrastructure Performance and Reliability, School of Engineering, The University of Newcastle, Callaghan, NSW 2308, Australia*

Received 10 July 2007; received in revised form 9 December 2007; accepted 21 December 2007

Available online 4 March 2008

## Abstract

A spatial time-dependent reliability model is developed for a RC beam subject to corrosion-induced pitting corrosion, for shear and flexural limit states. The analysis considers the spatial and time-dependent variability of pitting corrosion, structural resistance and load effects. The amount of corrosion loss can significantly affect the mechanical behaviour of reinforcement, namely low corrosion loss can result in ductile yielding, whereas a higher corrosion loss can result in brittle fracture. The progression from ductile to brittle behaviour is spatially and time-dependent. To estimate how such phenomena affects structural reliability the structural resistance of reinforcement is modelled as either (i) perfectly ductile parallel system or (ii) perfectly brittle parallel system. It was found that the probability of failure assuming brittle reinforcement behaviour is up to 450% higher than assuming ductile behaviour.

© 2008 Elsevier Ltd. All rights reserved.

*Keywords:* Pitting corrosion; Structural reliability; Spatial variability; Concrete; Ductility

## 1. Introduction

Pitting corrosion of reinforcing bars often occurs for Reinforced Concrete (RC) structures exposed to aggressive chloride environments (e.g., [1]). This highly localised form of steel corrosion can cause significant reductions in cross-section areas for reinforcing bars, for example, up to 80% loss of cross-section was observed for a 40-year-old Canadian bridge demolished in 1999 [2]. Pitting corrosion is non-homogeneous along a reinforcing bar, in fact it is highly spatially variable due to the spatial variability of concrete and steel material properties, environment, moisture, concrete cover, surface cracking, etc. While much work has progressed on the time-dependent structural reliability of deteriorating structures (e.g., [3–7]), much of this work assumes general (uniform) corrosion and if pitting corrosion is considered then simplifying assumptions are

often made, such as the maximum pit forms only at the location of maximum action or other critical location.

Recently, spatial variability of corrosion damage has been studied (e.g., [8–11]). This work has focused on corrosion-induced concrete cover cracking, and not on spatial variability of pitting corrosion and its effect on structural safety. However, Stewart [12] and Stewart and Al-Harthy [13] have modelled the spatial effect of pitting corrosion on the structural reliability of RC beams in flexure. Stewart [12] proposed a stochastic model of pitting corrosion for a simply supported RC office floor beam. The model used extreme value theory to predict maximum pit depth as a function of bar diameter and reinforcing bar length. This analysis made several assumptions: (i) statistics of pit depth variability taken from very limited experimental data obtained from the literature, (ii) ductile yielding of reinforcing bars, and (iii) influence of corrosion on material properties of steel reinforcing bar was not considered. Stewart and Al-Harthy [13] improved this work by using accelerated corrosion test data on 16 mm (Y16) and

\* Tel.: +61 2 49216027; fax: +61 2 49216991.

E-mail address: [mark.stewart@newcastle.edu.au](mailto:mark.stewart@newcastle.edu.au)

27 mm (Y27) diameter reinforcing steel bars to develop improved extreme value statistics for pitting and also included the effect of corrosion on reinforcement yield stress. Val [14] used the methodology and probabilistic pitting model derived by Stewart [12] to also consider the shear limit state. For large diameter reinforcement the use of ductile yielding may be appropriate, however, for small diameters such as for shear stirrups the assumption of ductile yielding will be shown to be inappropriate as brittle fracture is evident for severely corroded small diameter reinforcement (e.g., [15–17]).

The present paper improves the spatial time-dependent reliability analysis by considering shear and flexure limit states using improved probabilistic models of pitting described by Stewart and Al-Harthy [13], incorporating ductile and brittle mechanical behaviour of reinforcement for main (longitudinal) reinforcement and stirrups, and including statistics for time-dependent reduction in structural capacity and loss of cross-sectional area conditional on beam collapse. As will be shown herein, for most realistic structural and deterioration scenarios some reinforcement will fail by ductile yielding, and others by brittle fracture. The progression from ductile to brittle behaviour is spatially and time-dependent. To estimate how such phenomena affects structural reliability the structural resistance of reinforcement is modelled as either (i) perfectly ductile parallel system ( $p_{f\text{-ductile}}$ ) or (ii) perfectly brittle parallel system ( $p_{f\text{-brittle}}$ ). The actual structural reliability ( $p_f$ ) of a RC structural component will lie somewhere between these structural reliabilities such that  $p_{f\text{-ductile}} < p_f < p_{f\text{-brittle}}$ . The structural configuration considered is a simply supported RC beam comprising Y16 and Y27 main reinforcement and Y10 stirrups.

## 2. Probabilistic description of pitting for reinforcing bars

### 2.1. Pitting factor

A pitting factor  $R = p/P_{\text{av}}$  is used to define the extent of corrosion pitting, where  $p$  is the maximum pit depth and  $P_{\text{av}}$  is the penetration calculated based on general (uniform) corrosion ( $P_{\text{av}} = 0.0116i_{\text{corr}}t$ ). A Gumbel (EV-Type I) distribution is selected herein for modelling maximum pit depths for reinforcing bars. The use of the Gumbel distribution seems reasonable as extreme value statistics have been widely used to characterise pitting of steel plates and pipes and prestressing strands (e.g., [18–20]) and recently for Y16 and Y27 reinforcing bars [13]. To predict the distribution of maximum pitting factor for a reinforcing bar of length ( $L_U$ ), the Gumbel statistical parameters can be modified as [19]:

$$\mu = \mu_o + \frac{1}{\alpha_o} \ln \left( \frac{L_U}{L_o} \right) \quad (1)$$

$$\alpha = \alpha_o$$

where the Gumbel parameters  $\mu_o$  and  $\alpha_o$  are derived from statistical analysis of pitting data for reinforcement of length  $L_o$  (see Sections 2.1.1 and 2.1.2).

Note that the pitting factor  $R$  is assumed time-invariant, the distribution is truncated at  $R = 1$  and Eq. (1) assumes statistical independence between adjacent lengths. The assumption of statistical independence might not always be valid as the steel–concrete interface may not be totally independent between adjacent locations on a reinforcing bar, or even between bars. In the present case, however, statistics for pitting factors are taken from pit depths measured along and between reinforcing bars, and so the Gumbel parameters given above should help capture this variability. It has been observed that the pitting factor may reduce with time because as the size of the pit (anode) increases the ratio of anodic area to cathodic will reduce hence reducing the rate of depletion of the pit [16]. Hence, the statistics of pit depths proposed herein should be used with caution.

#### 2.1.1. Y10 rebars (stirrups)

Gonzalez et al. [21] found that for RC specimens exposed to natural environments the maximum pitting factor  $R$  varied from 4 to 8. These results were obtained for specimens with 8 mm diameter reinforcing bars of 125 mm length. The results of this study are in broad agreement with Tuutti [22]. Stewart [12] used this information to propose that the maximum pit depth for a 10 mm diameter reinforcing bar of 100 mm length of reinforcing steel is a Gumbel distribution with 5th and 95th percentiles being  $R = 4$  and  $R = 8$ , respectively. The statistical parameters for  $L_o = 100$  mm are given in Table 1.

#### 2.1.2. Y16 and Y27 rebars (main reinforcement)

Accelerated corrosion tests of two RC slabs provided spatial data on maximum pit depths for Y16 and Y27 rebars [13]. It was found that the Gumbel distribution provided the best fit for modelling maximum pit depths for reinforcing bars. Gumbel statistical parameters for pitting factors are shown in Table 1, for  $L_o = 100$  mm.

### 2.2. Effect of pitting on reinforcement cross-section

The maximum pit depth along a reinforcing bar of length  $L_U$  is

$$p(t) = 0.0116 \times i_{\text{corr}} \times R \times t \quad (2)$$

Table 1  
Statistics of pitting corrosion

Specimen	$L_o$ (mm)	Diameter (mm)	Pitting factor $R$		Gumbel parameters		Reference
			Mean	COV	$\mu_o$	$\alpha_o$	
Y10	100	10	5.65	0.22	5.08	1.02	[12]
Y16	100	16	6.2	0.18	5.56	1.16	[13]
Y27	100	27	7.1	0.17	6.55	1.07	[13]

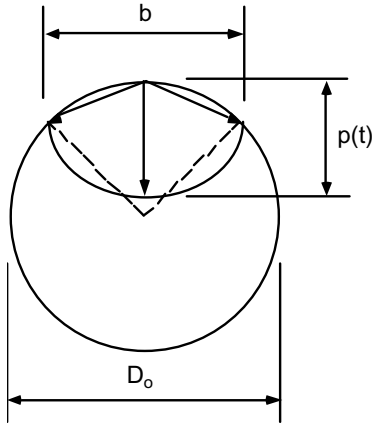


Fig. 1. Pit configuration.

where  $i_{\text{corr}}$  is the corrosion rate measured as a current density (normally expressed in  $\mu\text{A}/\text{cm}^2$ ),  $t$  is time since corrosion initiation in years and  $p(t)$  is in mm.

The pit configuration shown in Fig. 1 is used to predict the cross-sectional area of the pit ( $A_{\text{pit}}$ ), which can be expressed as [4]:

$$A_{\text{pit}}(t) = \begin{cases} A_1 + A_2 & p(t) \leq \frac{D_o}{\sqrt{2}} \\ \frac{\pi D_o^2}{4} - A_1 + A_2 & \frac{D_o}{\sqrt{2}} < p(t) \leq D_o \\ \frac{\pi D_o^2}{4} & p(t) \geq D_o \end{cases} \quad (3)$$

where

$$b = 2p(t) \sqrt{1 - \left(\frac{p(t)}{D_o}\right)^2}$$

$$A_1 = 0.5 \left[ \theta_1 \left(\frac{D_o}{2}\right)^2 - b \left| \frac{D_o}{2} - \frac{p(t)^2}{D_o} \right| \right]$$

$$A_2 = 0.5 \left[ \theta_2 p(t)^2 - b \frac{p(t)^2}{D_o} \right] \quad (4)$$

$$\theta_1 = 2 \arcsin \left( \frac{b}{D_o} \right) \quad \theta_2 = 2 \arcsin \left( \frac{b}{2p(t)} \right) \quad (5)$$

and where  $D_o$  is the initial diameter of the reinforcing bar. The cross-sectional area of an uncorroded reinforcing bar is

$$A_{\text{stnom}} = \pi \frac{D_o^2}{4} \quad (6)$$

### 2.3. Spatial capacity of reinforcing bars

There is sufficient evidence to suggest that yield stress reduces linearly with corrosion loss such that [23]:

$$f_y(t) = (1.0 - \alpha_y Q_{\text{corr}}(t)) f_{y0} \quad (7)$$

where  $f_{y0}$  is the yield stress of an uncorroded reinforcing bar,  $\alpha_y$  is an empirical coefficient, and  $Q_{\text{corr}}(t)$  is the percentage corrosion loss. Corrosion loss is measured in terms

of reduced cross-sectional area (or weight loss), hence Eq. (7) is re-expressed as

$$f_y(t) = \left( 1.0 - \alpha_y \frac{A_{\text{pit}}(t)}{A_{\text{stnom}}} \times 100 \right) f_{y0} \quad (8)$$

A review of 10 experimental studies [16] report average values of  $\alpha_y$  of up to 0.017. Du et al. [23] recommend that  $\alpha_y = 0.005$  and this value is used herein.

There is general consensus that the mechanical behaviour of reinforcing bars changes from ductile to non-ductile (brittle) as corrosion loss increases. What is less clear is the level of corrosion loss when the mechanical behaviour transitions from ductile to non-ductile behaviour and how this is affected by steel type. Almusallam [15] found brittle behaviour when corrosion loss ( $Q_{\text{corr}}$ ) exceeds 12.6% and others found complete loss of ductility when  $Q_{\text{corr}} = 20\%$  [16,17]. Palsson and Mirza [2] found that when  $Q_{\text{corr}} = 15\%$  there is a 33% reduction in ductility, and when  $Q_{\text{corr}}$  exceeds 50% corroded reinforcing bars are ‘‘very brittle’’. Apostolopoulos and Michalopoulos [24] observed that the additional plastic strain associated with corroded bent stirrups had significantly reduced ductility when compared to straight corroded stirrups (i.e., no bents). It has also been observed that corrosion of stirrups lead to a higher reduction in ductility [1].

While there is a gradual transition from ductile to brittle behaviour as corrosion loss increases, for the present paper it is conveniently assumed that complete loss of ductility in corroded reinforcing bars occurs after corrosion loss exceeds a threshold value of  $Q_{\text{limit}}$ . This leads to two types of mechanical behaviour dependent on corrosion loss:

$$\text{Ductile Behaviour : } Q_{\text{corr}} \leq Q_{\text{limit}} \quad (9)$$

$$\text{Brittle Behaviour : } Q_{\text{corr}} > Q_{\text{limit}}$$

From the above discussion it is reasonable to quantify  $Q_{\text{limit}} = 20\%$ , although more research is needed to more accurately quantify this important variable and its influencing factors.

For a spatial analysis a reinforcing bar is subdivided into equal lengths  $L_U$ , referred to herein as ‘uniform capacity length’, see Fig. 2. This length refers to the distance along a structural member in which localised corrosion will have a detrimental effect on structural capacity. The uniform capacity length is likely to be dependent on (i) the ability of corroded reinforcement to redistribute stresses to adjacent (less corroded) reinforcement via the concrete matrix, (ii) mechanical behaviour of the reinforcement (yield, brittle), (iii) development length of reinforcement (function of diameter of reinforcement and concrete cover) and (iv) geometry and spacing of reinforcement. The understanding of this phenomena is incomplete, with recent reliability studies assuming values of  $L_U$  varying from 100 mm to over 1000 mm [12–14]. This is clearly an area for further research and the present paper will investigate the effect of  $L_U$  on structural reliability in Section 5.2.2.

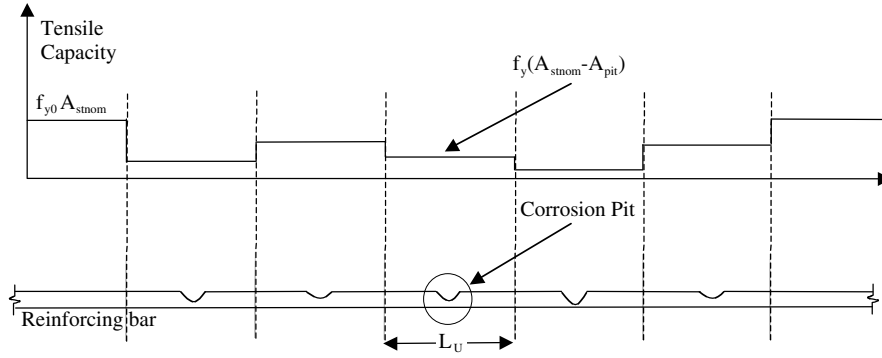


Fig. 2. Spatial capacity of corroded reinforcing bar showing uniform capacity length  $L_u$ .

### 3. Flexural and shear capacity for RC section

Strength prediction models used herein are based on code strength procedures, which are based on yield strength rather than ultimate tensile strength [16]. The use of yield capacity is verified when predicting ultimate moment and shear capacities for heavily corroded RC beams [17,25]. Thus, the section strength (and reinforcing bar capacity) is directly proportional to yield capacity – which is equal to the product of yield stress and cross-sectional area, both which are affected by pitting corrosion.

The reinforcement layout for a typical singly reinforced RC beam is shown in Fig. 3. The ultimate flexural capacity ( $M_u$ ) of a singly reinforced RC beam is

$$M_u = ME \times A_{st} f_y \left( d - \frac{A_{st} f_y}{1.7 f'_c b} \right) \quad (10)$$

which is a function of model error (ME), concrete compressive strength ( $f'_c$ ), effective depth ( $d$ ), beam width ( $b$ ), yield stress ( $f_y$ ) and cross-sectional area of reinforcement ( $A_{st}$ ) [26].

The ultimate shear capacity for beams with shear reinforcement ( $V_u$ ) comprises the shear capacity of concrete ( $V_c$ ) and shear reinforcement ( $V_s$ ):

$$V_u = V_c + V_s \quad (11)$$

where

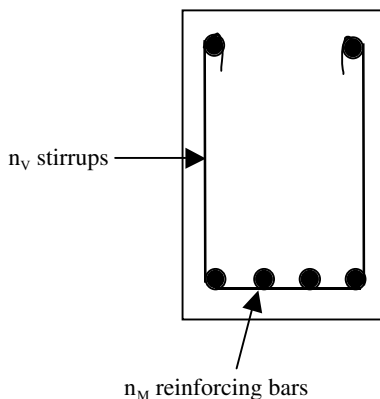


Fig. 3. Cross-section of RC beam.

$$V_c = ME_c \times 0.17 \sqrt{f'_c} b d \quad (12)$$

$$V_s = ME_s \times \frac{A_v f_y d}{s} = ME_s \times n_v A_v f_y \quad (13)$$

where  $A_v$  is the cross-sectional area of shear reinforcement (stirrup) with spacing  $s$  [26],  $n_v$  is the number of stirrups and  $ME_c$  and  $ME_s$  are model errors.

Since pitting corrosion only affects  $A_{st}$ ,  $A_v$  and  $f_y$  a near linear relationship exists between ultimate flexural and shear capacities and  $f_y A_{st}$  and  $f_y A_v$ , respectively. The effects of corrosion on reduction of bond and delamination or spalling of concrete cover are not considered.

Strength capacity of a RC section is based on a layout comprising of  $n$  reinforcing bars (e.g., main or shear reinforcement) and so it follows that these  $n$  reinforcing bars comprise a parallel system. For ductile behaviour there is equal load sharing between all reinforcement. However, brittle fracture will completely exhaust a reinforcing bars load-carrying capacity, resulting in load redistribution to the remaining bars, possibly leading to progressive failure of adjacent reinforcing bars. The strength prediction for a RC section ( $r$ ) is thus dependent on the mechanical behaviour of reinforcement and on the capacity of each reinforcing bar ( $r_i$ ), such that

$$\text{Perfectly Ductile Parallel System } r(t) = \sum_{i=1}^n r_i(t) \quad (14)$$

$$\text{Perfectly Brittle Parallel System } r(t) = \max(nr_1(t),$$

$$(n-1)r_2(t), \dots, 2r_{n-1}(t), r_n(t))$$

$$\text{where } r_1(t) < r_2(t) < \dots < r_n(t) \quad (15)$$

The capacity of a single reinforcing bar  $r_i$  is

$$\begin{aligned} r_i(t) &= f_y(t) A_i(t) \\ &= A_i(t) \left( 1.0 - \alpha_y \frac{A_{stnom} - A_i(t)}{A_{stnom}} \times 100 \right) f_{y0} \end{aligned} \quad (16)$$

where  $A_i(t)$  is the cross-sectional area of the  $i$ th reinforcing bar at time  $t$ . More details on the modelling of parallel systems are available elsewhere [27].

These analytical expressions will dramatically increase the computational efficiency of the analysis. Detailed numerical modelling (e.g., [17,28,29]) will lead to more

accurate estimates of structural capacities of corroding structures. However, even these analyses do not consider the spatial variability of pitting corrosion and the associated progressive failure of reinforcing bars and resulting load redistribution in the remaining reinforcing bars. These are areas for further study.

#### 4. Spatial time-dependent reliability analysis

##### 4.1. Discretisation of RC beam into elements

Figs. 4 and 5 show the discretisation of a RC beam into elements for flexure and shear limit states, respectively. The element length for flexure is the same as the uniform capacity length ( $L_U$ ). The failure mode for shear is diagonal cracking inclined at approximately  $45^\circ$  at locations of large shear force and small bending moment [30]. Hence, shear capacity is calculated for an element length  $\Delta_V = d$ . Note that these element lengths are bounded by physical properties of pitting corrosion (uniform capacity length) and structural capacity, and cannot be regarded as parameters (e.g., mesh size) that can be optimised to produce convergent results.

##### 4.2. Flexure and shear limit states

The critical limit state occurs when actual load effects exceed resistance at any element. In general, if it is assumed that  $K$  load events occur within the time interval  $(0, t_L)$  at times  $t_i$  ( $i = 1, 2, \dots, K$ ), then for this series system the critical flexural limit state for a beam comprising  $N_M$  elements is

$$G_{M,i}(X) = \min_{j=1, N_M} (M_j(t_i) - S_j(t_i)) \quad (17)$$

where  $M_j(t_1), M_j(t_2), \dots, M_j(t_K)$  represent the flexural resistance at the mid-point of each element and  $S_j(t_i)$  represents the bending moment at the mid-point of element  $j$  due to the  $i$ th load. The flexural resistance at any element  $j$  at time  $t$  is

$$M_j(t) \approx \frac{r_j(t)}{n_M f_y 0 A_{stnom}} M_u \quad (18)$$

where  $r_j(t)$  is obtained from Eqs. (14) or (15) for  $n_M$  reinforcing bars, see Fig. 4.

Similarly, the critical shear limit state for a beam comprising  $N_V$  elements is

$$G_{V,i}(X) = \min_{k=1, N_V} (V_k(t_i) - S_k(t_i)) \quad (19)$$

where  $V_k(t_1), V_k(t_2), \dots, V_k(t_K)$  represent the shear resistance at the mid-point of each element and  $S_k(t_i)$  represents the shear force at the mid-point of element  $k$  due to the  $i$ th load. The shear resistance at any element  $k$  at time  $t$  is thus

$$V_j(t) \approx V_c + \frac{r_k(t)}{n_V f_y 0 A_{stnom}} V_s \quad (20)$$

where  $r_k(t)$  is obtained from Eqs. (14) or (15) for  $n_V$  stirrups, see Fig. 5.

If flexure and shear are considered, then the critical combined limit state is

$$G_{t_i}(X) = \min[G_{M,t_i}(X), G_{V,t_i}(X)] \quad (21)$$

The cumulative probabilities of failure for flexure ( $p_{FM}$ ), shear ( $p_{FV}$ ) and combined ( $p_F$ ) limit states anytime during this time interval are, respectively

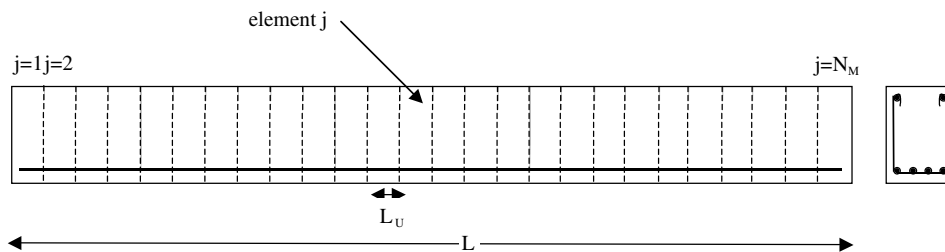


Fig. 4. Discretisation of RC beam, for flexure.

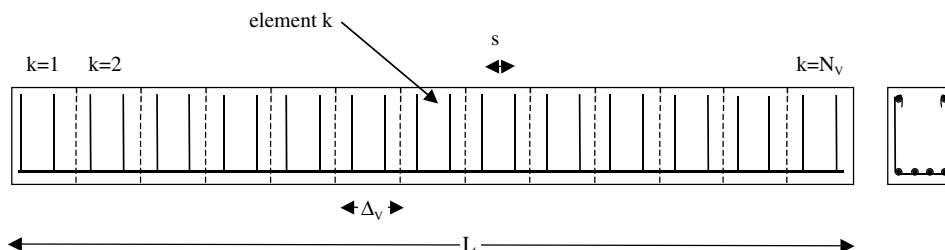


Fig. 5. Discretisation of RC beam, for shear with  $s/d = 0.5$ .

$$p_{FM}(0, t_L) = 1 - \Pr[G_{M,t_1}(X) > 0 \cap G_{M,t_2}(X) > 0 \cap \dots \cap G_{M,t_K}(X) > 0] \quad t_1 < t_2 < \dots < t_K \leq t_L \quad (22)$$

$$p_{FV}(0, t_L) = 1 - \Pr[G_{V,t_1}(X) > 0 \cap G_{V,t_2}(X) > 0 \cap \dots \cap G_{V,t_K}(X) > 0] \quad t_1 < t_2 < \dots < t_K \leq t_L \quad (23)$$

$$p_f(0, t_L) = 1 - \Pr[G_{t_1}(X) > 0 \cap G_{t_2}(X) > 0 \cap \dots \cap G_{t_K}(X) > 0] \quad t_1 < t_2 < \dots < t_K \leq t_L \quad (24)$$

For deteriorating structures the deterioration process will reduce structural resistance and so structural resistance is time-dependent. This represents a first passage probability.

It is often assumed by other researchers, often for computational convenience, that failure events are independent events, which leads to

$$p_f(0, t_L) \approx 1 - \prod_{i=1}^K [1 - \Pr(G_{t_i}(X) \leq 0)] \quad (25)$$

However, the assumption of independence of failures in different years overestimates the probability of failure [6]. Eq. (25) may provide a good approximation for some high reliability problems. On the other hand, the accuracy decreases as the coefficient of variation of resistance increases, which is relevant for deteriorating structures as they tend to have high variability of resistance due to spatial and temporal uncertainties of corrosion phenomena. For example, Stewart and Al-Harthy [13] observed that the approximate solution given by Eq. (25) overestimated the probability of failure calculated from Eq. (22) by more than 80% for typical RC beams subject to reinforcement corrosion. Hence, there is ample evidence to suggest that Eq. (25) is a poor approximation of the more accurate first passage probabilities given by Eqs. (22)–(24) for deteriorating structures and so Eq. (25) is not used herein.

#### 4.3. Spatial and time-dependent mechanical behaviour of reinforcement

Eqs. (14) and (15) show that the mechanical behaviour of reinforcing bars can significantly affect structural capacity. The mechanical behaviour for all main reinforcement and stirrups in a RC beam cannot be predicted ‘a priori’. However, it is possible to predict the probability that at least one reinforcing bar in a RC section (or element) comprising  $n$  reinforcing bars is brittle at time  $t$ , denoted herein as  $\Pr(\text{brittle}, t)$ . If  $\Pr(\text{brittle}, t)$  is high then the assumption that all reinforcing bars exhibit ductile behaviour is not valid, and that the mechanical behaviour for some or all reinforcing bars is brittle. The derivation of  $\Pr(\text{brittle}, t)$  is

$$\begin{aligned} \Pr(\text{brittle}, t) &= \Pr(\text{at least one rebar is brittle}) \\ &= 1 - \Pr(\text{all rebars are ductile}) \\ &= 1 - [\Pr(\text{one rebar is ductile})]^n \\ &= 1 - [\Pr(Q_{\text{corr}}(t) < Q_{\text{limit}})]^n \end{aligned} \quad (26)$$

If for the sake of illustration the probability distribution of  $Q_{\text{corr}}(t)$  is assumed normally distributed and the corrosion loss for each reinforcing bar is assumed statistically independent, then

$$\Pr(\text{brittle}, t) \approx 1 - \left[ \Phi \left( \frac{Q_{\text{limit}} - \lambda(t)}{\sigma(t)} \right) \right]^n \quad (27)$$

where  $\Phi()$  is the standard Normal distribution function,  $\lambda(t)$  and  $\sigma(t)$  are the mean and standard deviation of the distribution of  $Q_{\text{corr}} (=A_{\text{pit}}(t)/A_{\text{stnom}})$  for a single reinforcing bar of uniform capacity length  $L_U$  at time  $t$ ,  $Q_{\text{limit}}$  is the corrosion loss when brittle behaviour occurs ( $=20\%$ ) and  $n$  is the number of reinforcing bars used to calculate section capacity. The probability distribution of  $Q_{\text{corr}}$  is dependent on the random variability of corrosion rate and pitting factor  $R$  (Eq. (1)). To be sure, the estimate of  $\Pr(\text{brittle}, t)$  could be obtained by more accurate methods (such as simulation). The assumption implicit in most reliability analyses of deteriorating structures is that all corroding reinforcement will behave in a ductile manner, so the intent of the present section is to simply show that such an assumption may seldom be correct for many deteriorating structures.

Fig. 6 shows the mean proportional loss of cross-section  $\lambda(t)$  for Y10, Y16 and Y27 reinforcement for deterministic corrosion rates of  $0.5 \mu\text{A}/\text{cm}^2$ ,  $1 \mu\text{A}/\text{cm}^2$  and  $2 \mu\text{A}/\text{cm}^2$ . As expected,  $\lambda(t)$  increases as the reinforcing bar diameter reduces or as the corrosion rate increases. Given the high variability of pitting factor the coefficient of variation (COV) of  $Q_{\text{corr}}$  is significant, varying from 0.13 to 0.30. Eq. (27) and data from Fig. 6 are then used to calculate the time-dependent probabilities that at least one reinforcing bar in a RC section is brittle  $\Pr(\text{brittle}, t)$  for Y10, Y16 and Y27 reinforcement for corrosion rates of  $1 \mu\text{A}/\text{cm}^2$  and  $2 \mu\text{A}/\text{cm}^2$  and  $n = 2, 6, 10, 20$  (see Figs. 7 and 8). Note that  $\Pr(\text{brittle}, t) \approx 0$  for  $i_{\text{corr}} = 0.5 \mu\text{A}/\text{cm}^2$ . For corrosion rates of  $1 \mu\text{A}/\text{cm}^2$  or higher Figs. 7 and 8 show there is a high likelihood that the mechanical behaviour of Y10 reinforcement is not ductile. This likelihood increases with the number of reinforcing bars and time since corrosion initiation. As the diameter of reinforcement increases the likelihood

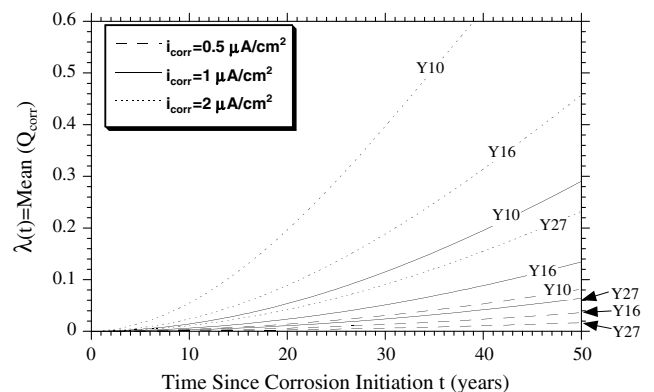


Fig. 6. Mean corrosion loss for  $L_U = 500$  mm.

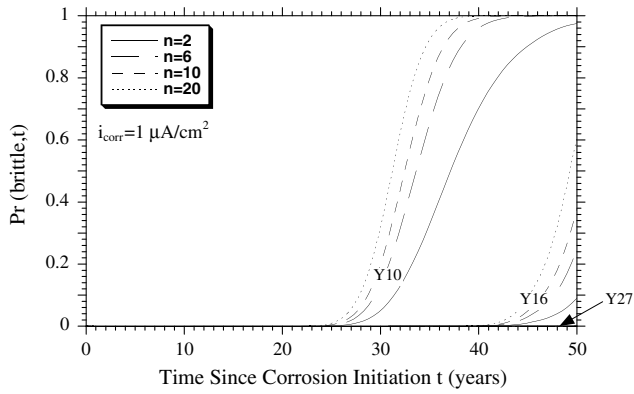


Fig. 7. Probability that some reinforcement exhibits brittle behaviour, for  $Q_{\text{limit}} = 20\%$ ,  $i_{\text{corr}} = 1 \mu\text{A}/\text{cm}^2$  and  $L_U = 500 \text{ mm}$ .

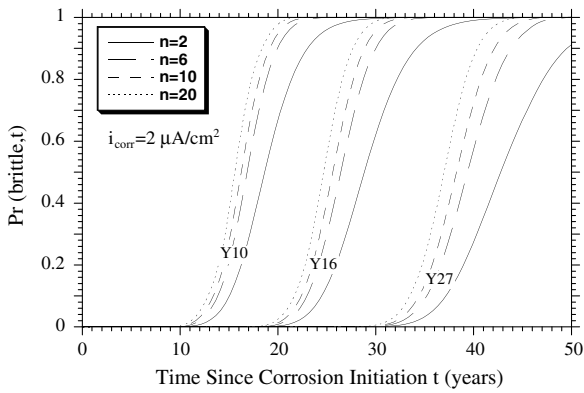


Fig. 8. Probability that some reinforcement exhibits brittle behaviour, for  $Q_{\text{limit}} = 20\%$ ,  $i_{\text{corr}} = 2 \mu\text{A}/\text{cm}^2$  and  $L_U = 500 \text{ mm}$ .

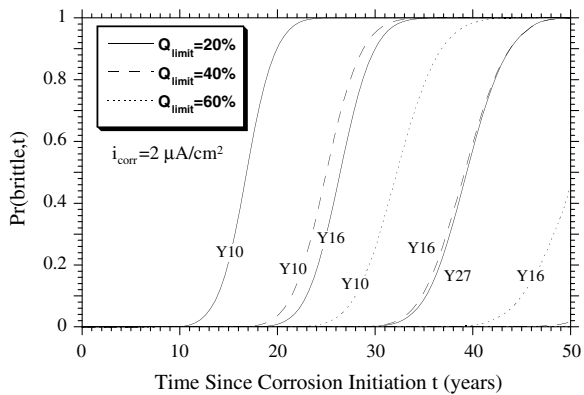


Fig. 9. Effect of corrosion loss limit ( $Q_{\text{limit}}$ ) on probability that some reinforcement exhibits brittle behaviour, for  $i_{\text{corr}} = 2 \mu\text{A}/\text{cm}^2$ ,  $n = 6$  and  $L_U = 500 \text{ mm}$ .

of brittle behaviour decreases. Fig. 9 shows that brittle behaviour of some reinforcement is still likely even if the corrosion loss limit between ductile and brittle behaviour ( $Q_{\text{limit}}$ ) is increased from 20% to 40% or 60%, for  $i_{\text{corr}} = 2 \mu\text{A}/\text{cm}^2$ .

Figs. 7 and 8 clearly show that in a RC structural component that comprises of many reinforcing bars and elements

there is a strong likelihood of non-ductile behaviour in at least one corroding reinforcing bar irrespective of structural configuration (with the possible exception of very low corrosion rates). Hence, some reinforcement which is more heavily corroded than other reinforcement will exhibit brittle behaviour, and other (less corroded) reinforcement ductile behaviour. Clearly, this phenomena is very difficult to model either numerically or by stochastic FEA. In light of such difficulties, it is reasonable to assume two bounds on structural reliability, namely, all reinforcement in a RC structural component exhibits: (i) ductile behaviour ( $p_{f\text{-ductile}}$ ) or (ii) brittle behaviour ( $p_{f\text{-brittle}}$ ). As the capacity of a perfectly brittle parallel system is less than that of a perfectly ductile parallel system, it follows that the actual structural reliability ( $p_f$ ) of the RC structural component will thus lie somewhere between these structural reliabilities such that  $p_{f\text{-ductile}} < p_f < p_{f\text{-brittle}}$ .

#### 4.4. Computational method

Monte-Carlo simulation is used herein to calculate  $p_{f\text{-ductile}}$  and  $p_{f\text{-brittle}}$  which are based on an evaluation of Eqs. (22)–(24). A reinforcing bar will be subject to multiple pits, and the deepest pit (Gumbel distribution described by Eqs. (1) and (2)) is assumed to occur in the middle of each element. Hence the capacity of an element is taken at the cross-section of the middle of the element. For each simulation run, the pitting factor ( $R$ ) for each reinforcing bar in each element is randomly generated at  $t = 0$ . The maximum pit depths and remaining cross-sectional areas of reinforcing steel are then inferred from Eqs. (2)–(5). The flexural and shear resistances of the same (randomly generated) beam are then calculated at each time interval for elements  $j$  and  $k$ , respectively. The applied loads are then randomly generated for the time increment and the flexure and shear load effects calculated for each element  $j$  and  $k$ . The limit state functions given by Eqs. (17), (19) and (21) are then checked for all elements. This process continues for successive annual time increments and elements until failure occurs ( $G_{ti} < 0$ ) or until its service life is reached. At the completion of all simulation runs, the cumulative probabilities of failure given by Eqs. (22)–(24) are inferred at each time increment. An advantage of Monte-Carlo simulation is its ability to infer intermediate statistics on system performance, such as statistics on resistance and corrosion loss at time of failure.

### 5. Example structural configuration

#### 5.1. RC beam

The structural configuration is a simply supported RC beam with cross-section given by Fig. 3. The nominal (or design) capacity of an uncorroded RC beam is denoted as  $M_{\text{nom}}$  and  $V_{\text{nom}}$  for flexure and shear, respectively. In the present case, the nominal resistance in RC design is obtained from the design condition  $\phi R_{\text{nom}} = 1.2G_n + 1.6Q_n$

[26] where  $\phi = 0.9$  and  $\phi = 0.75$  for flexure and shear, respectively. It follows that nominal flexural and shear capacities are  $M_{\text{nom}} = (1.2G_n + 1.6Q_n)/0.9$  and  $V_{\text{nom}} = (1.2G_n + 1.6Q_n)/0.75$ , respectively. The nominal capacity depends on the live-to-dead load ratio  $\rho = Q_n/G_n$  where  $G_n$  and  $Q_n$  are design dead and live loads respectively. For shear design, the ratio  $V_s/V_c$  is used to denote the ratio of nominal (or design) concrete ( $V_{\text{cnom}}$ ) to reinforcement shear ( $V_{\text{snom}}$ ) capacities.

The ultimate-to-nominal flexural resistance ( $M_u/M_{\text{nom}}$ ) for a RC beam is modelled as a normal distribution with mean of 1.135 and COV of 0.085 [31]. These statistics include the random variability of  $ME$ ,  $A_{\text{st}}$ ,  $f'_c$ ,  $f_y$ ,  $b$  and  $d$  as defined in Eq. (10). The ultimate-to-nominal shear resistance provided by concrete ( $V_c/V_{\text{cnom}}$ ) is normally distributed with mean of 1.22 and COV of 0.20 [31]. The ultimate-to-nominal shear resistance provided by shear reinforcement ( $V_s/V_{\text{snom}}$ ) is inferred from Nowak et al. [31] as being normally distributed with mean of 1.2 and COV of 0.15. These shear statistics include the random variability of  $ME_c$ ,  $ME_s$ ,  $A_v$ ,  $f'_c$ ,  $f_y$ ,  $b$ ,  $s$  and  $d$  as defined in Eqs. (12) and (13).

Statistical parameters for a stochastic office floor load are shown in Table 2. The load effects from these uniformly distributed loads produces a bending moment ( $S_j$ ) and shear force ( $S_k$ ) which is obviously spatially variable. The time period is taken as 50 years, with extraordinary live load effects updated annually and sustained live load effects updated every 8 years resulting in  $K = 50$  load events.

While the structural configuration considered herein is a RC beam assuming stochastic office floor loading, the RC section shown in Fig. 3 is appropriate also for bridges, car-parks, wharf structures and a range of other RC structures. The reliability of these structures would be similar to that for commercial structures, and so the results presented herein can be generalised to a range of RC structures exposed to aggressive environments.

The mean corrosion current density ( $i_{\text{corr}}$ ) can vary significantly (see Table 3), however, for the present paper  $i_{\text{corr}} = 1 \mu\text{A}/\text{cm}^2$  is used as a “medium corrosion intensity” estimate. Corrosion rate is influenced by concrete properties and cover (e.g., [10,32]). Since there is random variability of concrete properties and cover, Vu [33] suggested that the COV for corrosion rate can vary from 0.25 to 0.60 for typical covers and concrete strengths. This is in broad agreement with Enright and Frangopol [34] who suggested a COV of 0.3 based on the range reported for corroded

Table 3  
Typical corrosion rates for RC structures in  $\mu\text{A}/\text{cm}^2$

Classification	Andrade and Alonso [40]	Dhir et al. [41]	BRITE/EURAM [42]	Roberts et al. [43]
Negligible	<0.1	–	<0.1	–
Low	0.1–1.0	0.1	0.1–0.5	<0.2
Medium	1.0–10	1	0.5–1.0	0.2–1.0
High	10–100	10	>1.0	>1.0

bridges. Thus, corrosion rate is assumed normally distributed with a COV of 0.3. In principle, other parameters such as concrete strength and cover, etc. could also have been modelled as spatial variables which in turn would further influence  $M_j(t_i)$  and  $V_k(t_i)$ . Gumbel parameters for the pitting factor used in Eq. (1) are taken from Table 1.

Section 2.3 found that there are a number of difficulties in quantifying the uniform capacity length  $L_U$ , with previous researchers assuming  $L_U$  from 100 mm to over 1000 mm. For this reason, the uniform capacity length  $L_U$  for main reinforcement is assumed to be 125 mm, 250 mm, 500 mm or 1000 mm to assess the sensitivity of flexural structural reliabilities ( $p_{\text{FM}}$ ) to  $L_U$ . On the other hand, shear diagonal cracking can occur anywhere along a stirrup within an element, so in this case the maximum pit along a stirrup is obtained using  $L_U = \text{length of stirrup}$ .

The baseline case for subsequent analyses is a RC beam with  $L/d = 12$  as this is typical in practice with  $L = 8$  m,  $n_M = 6$  main reinforcing bars, stirrup spacing of  $s/d = 0.5$  ( $n_V = 2$ ),  $\alpha_y = 0.005$ ,  $i_{\text{corr}} = 1 \mu\text{A}/\text{cm}^2$ ,  $L_U = 500$  mm for main reinforcement and stirrups, and  $\Delta_V = d$ . The purpose of the structural reliability analysis is comparative only. They should not be interpreted in an absolute sense.

## 5.2. Results

It has been shown that probabilities of failure considering spatial variability of pitting corrosion were up to 200% higher than probabilities of failure obtained from a non-spatial analysis [12,13]. Hence, the importance of considering spatial variability in a structural reliability analysis for deteriorating structures is well documented and proven. The analyses presented herein will consider the effect of limit state, corrosion loss, uniform capacity length, reinforcing bar diameter and number of reinforcing bars on time-dependent structural reliability. The live-to-dead load ratio ( $\rho = 0.5$ – $1.5$ ) and the reinforcement ratio ( $V_s/V_c = 0.5$ – $1.5$ ) did not affect the overall trend of the results presented herein, hence results to follow are for  $\rho = 1.0$  and  $V_s/V_c = 1.0$ .

Note that the reliability index ( $\beta$ ) after 50 years, assuming no deterioration, is 3.51. This is consistent with target reliability indices for RC members for buildings and bridges, and shows that the resistance and load modelling is consistent with that experienced by RC members in general.

Table 2  
Load model statistics

Load	Duration	Mean	COV	Distribution	Reference
Dead load	Permanent	$1.05G_n$	0.10	Normal	[35]
<i>Live load</i>					
Sustained	8 Years	$0.30Q_n$	0.60	Gamma	[36,37]
Extraordinary	1 Year	$0.19Q_n$	0.66	Gamma	[38]

Note:  $G_n$ ,  $Q_n$  design loads specified from ANSI/ASCE 7 [39].

5.2.1. Effect of mechanical behaviour on structural resistance and reliability

The effect of mechanical behaviour on the time-dependent reduction in flexural and shear capacities for any element are shown in Fig. 10. In this case, mean capacity based on brittle behaviour is up to 9% less than that predicted from ductile behaviour. Moreover, the COV of capacity increases by up to 25% for brittle behaviour. Fig. 11 shows how mechanical behaviour affects the governing (critical) limit state, and that the governing limit state is not always at the region of peak actions (mid-span for flexure, support for shear). Since capacity is reduced for brittle behaviour (see Fig. 10), the governing limit state for brittle behaviour is more likely to occur in an element with reduced structural action (e.g. reduced bending moment), resulting in governing limit states being further away from the element with the peak structural action. The observations made from Figs. 10 and 11 all suggest that assuming brittle behaviour for all reinforcement in a RC section will lead to higher probabilities of failure.

Fig. 12 shows the cumulative probabilities of failure for ductile behaviour ( $p_{f-ductile}$ ) and brittle behaviour ( $p_{f-brittle}$ ), for flexure, shear and combined limit states. The probabilities of failure considering all reinforcement to exhibit brittle behaviour are up to 450% higher than probabilities of failure assuming all reinforcement exhibits ductile behaviour. Clearly, the mechanical behaviour of reinforcement has a significant effect on structural reliability, and the bounds on the actual probability of failure  $p_{f-ductile} < p_f < p_{f-brittle}$  can be considerable after as little as 15–20 years of corrosion.

Stewart [12] showed that the variability of structural resistance of reinforcement subject to ductile behaviour increases as the number of reinforcing bar decreases, leading to higher probabilities of failure. For example, the present analysis shows that reducing Y16 reinforcement from 10 to 2 bars increases the probability of flexural failure by 100%. However, for brittle behaviour, the resistance given by Eq. (17) is related to the variability of the weakest reinforcement. Hence, as the number of reinforcing bars

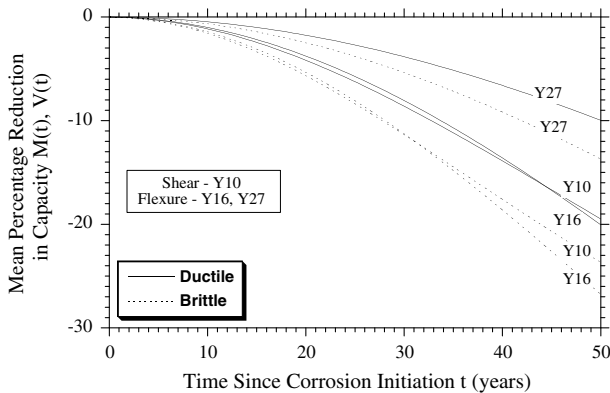


Fig. 10. Time-dependent percentage reduction in mean flexural and shear capacities.

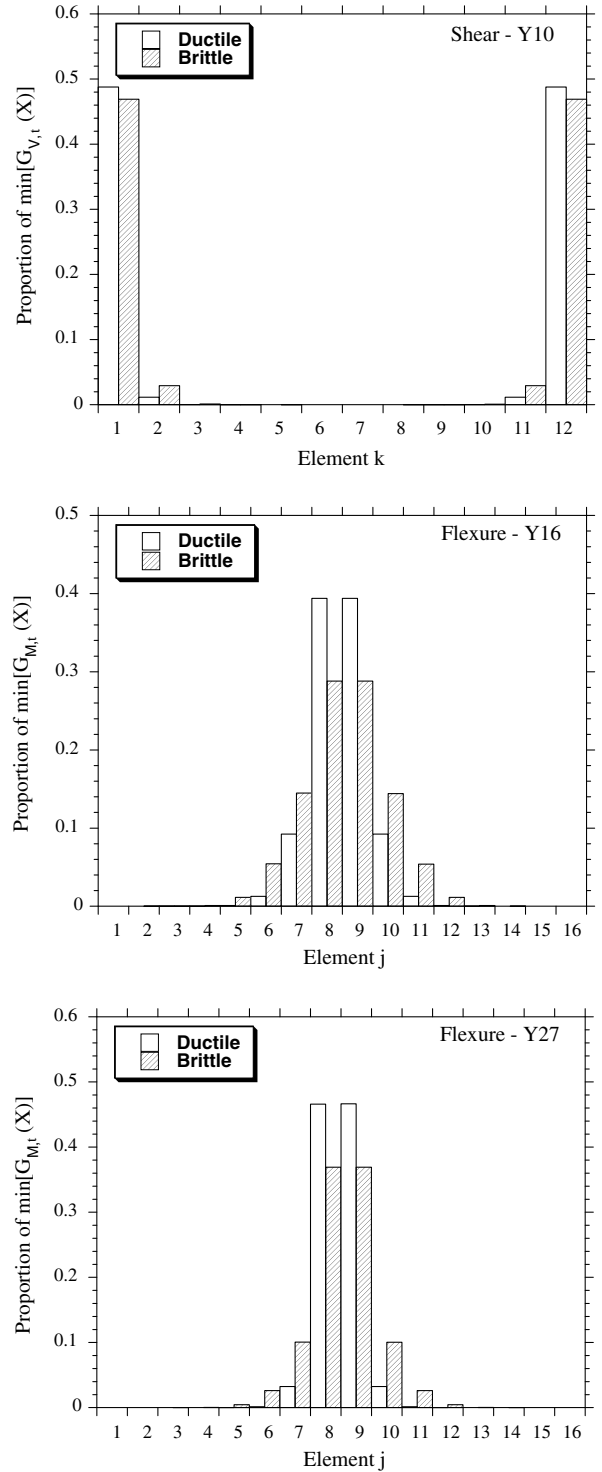


Fig. 11. Effect of reinforcement mechanical behaviour on distribution of spatial position of governing limit state over 50 years of pitting corrosion.

increases, the likelihood of deeper pits increase, leading to reduced section capacity and higher probabilities of failure. However, the present analysis shows that this increase is marginal; for example, increasing Y16 reinforcement (assuming brittle behaviour) from 2 to 10 bars reduces the probability of flexural failure by less than 15%. Hence,

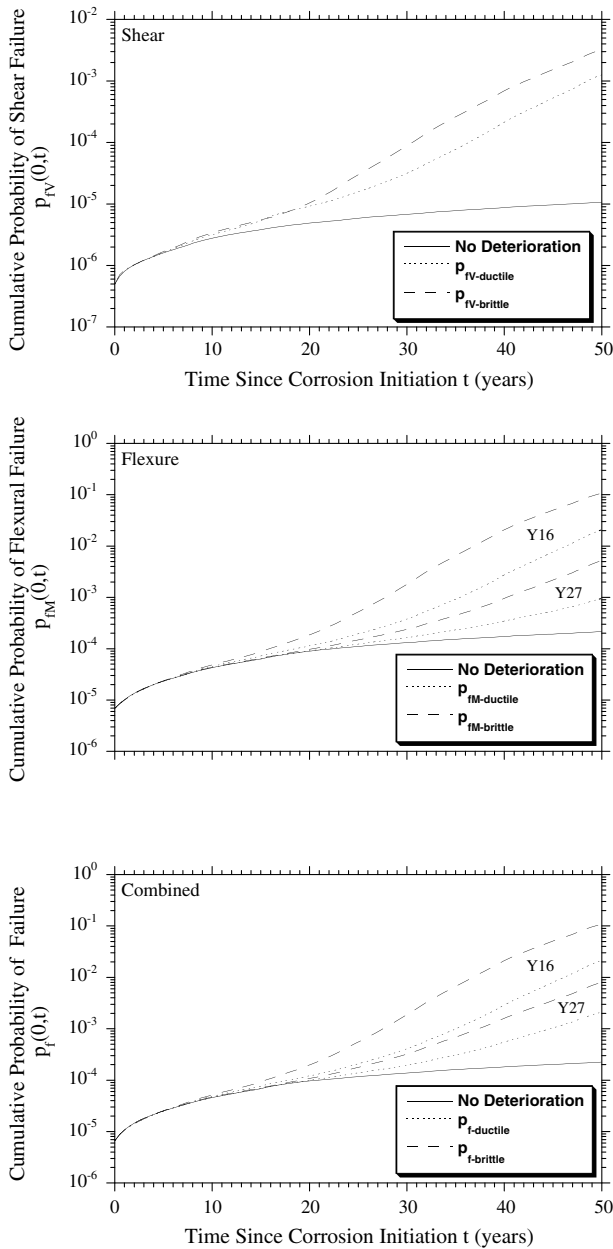


Fig. 12. Cumulative probabilities of failure showing  $p_{f-ductile}$  and  $p_{f-brittle}$  for flexure, shear and combined limit states.

the number of reinforcing bars in a RC section has the greatest influence on structural reliability for ductile mechanical behaviour.

5.2.2. Effect of uniform capacity length on structural resistance and reliability

Eq. (1) shows that the uniform capacity length  $L_U$  is a key parameter in the Gumbel distribution of pitting factor. As  $L_U$  increases the mean pitting factor increases, leading to an increased reduction in flexural capacity as  $L_U$  increases from 125 mm to 1000 mm (see Fig. 13). It is also apparent that the difference between mean flexural capacity for ductile and brittle behaviour is approximately 5–9%.

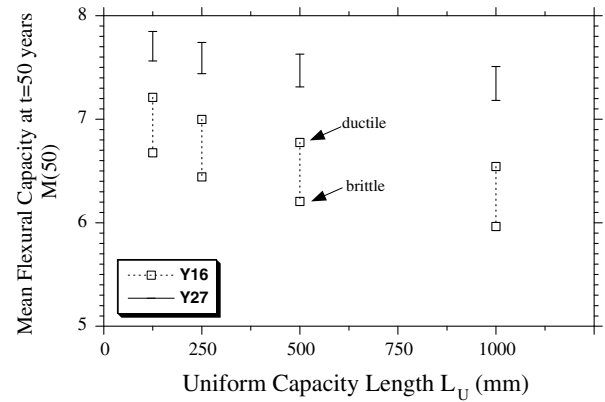


Fig. 13. Effect of uniform capacity length on mean flexural capacity at  $t = 50$  years.

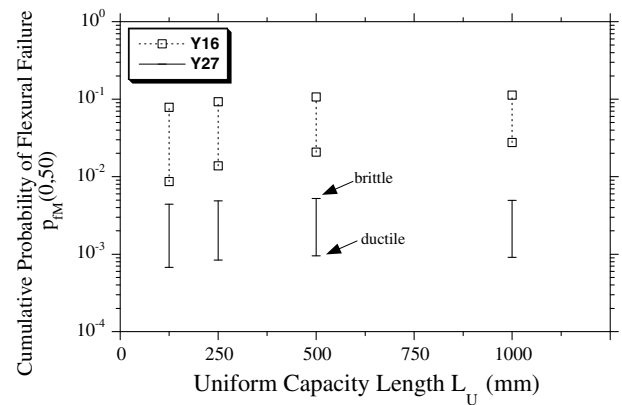


Fig. 14. Effect of uniform capacity length on cumulative probability of flexural failure at  $t = 50$  years.

Note that in the present paper  $L_U$  for stirrups is fixed at 500 mm, so the effect of  $L_U$  on structural resistance and reliability is investigated for the flexural limit state only.

Fig. 14 shows that cumulative probability of flexural failure at  $t = 50$  years can be quite sensitive to  $L_U$ . As this is a series system, it might be expected that more elements (reduced  $L_U$ ) would cause an increase in probability failure; however, this effect is outweighed by the observation in Fig. 13 that as  $L_U$  increases the capacity of an element decreases. It is for this reason that Fig. 14 shows that cumulative probability of flexural failure increases as  $L_U$  increases. This trend may not always be observed (e.g., Y27 when  $L_U = 1000$  mm), however, since load effect ( $S_j$ ) is taken at the midpoint of an element, which will decrease as  $L_U$  increases. As discussed in Section 2.3, the quantification of  $L_U$  for RC sections containing multiple reinforcing bars, each with spatially variable pitting corrosion, is a difficult and complex phenomenon to model. More research is needed to better understand this phenomenon, which may include a time or event-based non-linear FEA to progressively track the redistribution of loads between and along adjacent reinforcement considering the pitting and mechanical behaviour of reinforcement.

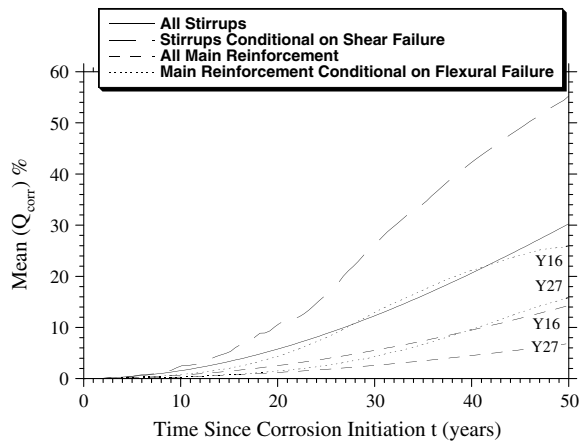


Fig. 15. Average corrosion loss at time of shear and flexural failure.

### 5.2.3. Statistics of corrosion loss

Finally, Fig. 15 shows the average corrosion loss for all reinforcement, and the average corrosion loss in an element conditional on exceeding the flexure or shear limit state. It is observed from Fig. 15 that at the time of shear failure the average corrosion loss of stirrups is in excess of 50% after 50 years. The average corrosion loss is reduced for main reinforcement (due to its larger bar diameter), but is still significant. The variability of corrosion loss for all reinforcement is also very high, often with a COV in excess of 0.5. This is not unexpected due to the highly variable nature of the spatial and temporal characteristics of resistance and load.

## 6. Conclusions

An improved spatial time-dependent reliability analysis is developed for a RC beam subject to corrosion-induced pitting corrosion, for shear and flexural limit states. The analysis considered the spatial and time-dependent variability of pitting corrosion, structural resistance and load effects. The effect of the mechanical behaviour of reinforcement, corrosion rate and uniform capacity length on structural resistance and reliability are presented. It was found that the probability of failure assuming brittle reinforcement behaviour is up to 450% higher than assuming ductile behaviour. It was also found that the length of reinforcement needed to distribute loads from severely corroded reinforcement to adjacent reinforcement (uniform capacity length) has a significant effect on structural reliability. The results show that including mechanical behaviour of reinforcement subject to pitting corrosion is an important consideration when calculating structural reliabilities of corroding RC structures.

## Acknowledgements

Part of this work was undertaken while the author was on sabbatical leave at Ohio State University. The author appreciates the support of the Department of Civil and

Environmental Engineering and Geodetic Sciences at Ohio State University. The support of the Australian Research Council is gratefully acknowledged.

## References

- [1] Higgins C, Farrow WC. Tests of reinforced concrete beams with corrosion-damaged stirrups. *ACI Struct J* 2006;103(1):133–41.
- [2] Palsson R, Mirza MS. Mechanical response of corroded steel reinforcement of abandoned concrete bridge. *ACI Struct J* 2002;99(2):157–62.
- [3] Mori Y, Ellingwood BR. Reliability-based service-life assessment of aging concrete structures. *J Struct Eng, ASCE* 1993;119(5):1600–21.
- [4] Val DV, Melchers RE. Reliability of deteriorating RC slab bridges. *J Struct Eng, ASCE* 1997;123(12):1638–44.
- [5] Vu KAT, Stewart MG. Structural reliability of concrete bridges including improved chloride-induced corrosion models. *Struct Safety* 2000;22(4):313–33.
- [6] Val D, Stewart MG, Melchers RE. Life-cycle performance of reinforced concrete bridges, probabilistic approach. *J Comput Aided Civil Infrastruct Eng* 2000;15(1):14–25.
- [7] Estes AC, Frangopol DM. Bridge lifetime system reliability under multiple limit states. *J Bridge Eng, ASCE* 2001;6(6):523–8.
- [8] Li Y, Vrouwenvelder T, Wijnants GH, Walraven J. Spatial variability of concrete deterioration and repair strategies. *Struct Concrete* 2004;5(3):121–30.
- [9] Malioka V, Faber MH. Modeling of the spatial variability for concrete structures, bridge maintenance, safety, management and cost. In: Watanabe E, Frangopol DM, Utsunomiya T, editors, *IABMAS'04*, A.A. Balkema, Rotterdam (CD-ROM); 2004.
- [10] Vu KAT, Stewart MG. Predicting the likelihood and extent of RC corrosion-induced cracking. *J Struct Eng, ASCE* 2005;131(11):1681–9.
- [11] Stewart MG, Mullard JA. Spatial time-dependent reliability analysis of corrosion damage and the timing of first repair for RC structures. *Eng Struct* 2007;29(7):1457–64.
- [12] Stewart MG. Spatial variability of pitting corrosion and its influence on structural fragility and reliability of RC beams in flexure. *Struct Safety* 2004;26(4):453–70.
- [13] Stewart MG, Al-Harthy A. Pitting corrosion and structural reliability of corroding RC structures, experimental data and probabilistic analysis. *Reliab Eng Syst Safety* 2008;93(3):273–382.
- [14] Val DV. Deterioration of strength of RC beams due to corrosion and its influence on beam reliability. *J Struct Eng, ASCE* 2007;133(9):1297–306.
- [15] Almusallam AA. Effect of degree of corrosion on the properties of reinforcing steel bars. *Construct Build Mater* 2001;15:361–8.
- [16] Cairns J, Plizzari GA, Du Y, Law DW, Franzoni C. Mechanical properties of corrosion-damaged reinforcement. *ACI Mater J* 2005;102(4):256–64.
- [17] Coronelli D, Gambarova P. Structural assessment of corroded reinforced concrete beams: modeling guidelines. *J Struct Eng, ASCE* 2004;130(8):1214–24.
- [18] Hawn DE. Extreme value prediction of maximum pits on pipelines. *Mater Perform* 1977;29–32.
- [19] Sheikh AK, Boah JK, Hansen DA. Statistical modelling of pitting corrosion and pipeline reliability. *Corrosion-NACE* 1990;46(3):190–7.
- [20] Darmawan MS, Stewart MG. Spatial time-dependent reliability analysis of corroding pretensioned prestressed concrete bridge girders. *Struct Safety* 2007;29(1):16–31.
- [21] Gonzalez JA, Andrade C, Alonso C, Feliu S. Comparison of rates of general corrosion and maximum pitting penetration on concrete embedded steel reinforcement. *Cement Concrete Res* 1995;25(2):257–64.
- [22] Tuutti K. Corrosion of steel in concrete. Swedish Cement and Concrete Research Institute, Fo 4.82, Stockholm; 1982.

- [23] Du YG, Clark LA, Chan AHC. Residual capacity of corroded reinforcing bars. *Mag Concrete Res* 2005;57(3):135–47.
- [24] Apostolopoulos CA, Michalopoulos D. The impact of corrosion on the mechanical behaviour of steel undergoing plastic deformation. *Mater Corros* 2007;58(1):5–12.
- [25] Rodriguez J, Ortega LM, Casal J. Load carrying capacity of concrete structures with corroded reinforcement. *Construct Build Mater* 1997;11(4):239–48.
- [26] ACI 318. Building code requirements for structural concrete. Detroit, Michigan: ACI; 2005.
- [27] Thoft-Christensen P, Baker MJ. Structural reliability theory and its applications. Berlin: Springer-Verlag; 1982.
- [28] El Maaddawy TE, Soudki K, Topper T. Analytical model to predict nonlinear flexural behaviour of corroded reinforced concrete beams. *ACI Struct J* 2005;102(4):550–9.
- [29] Tastani S, Pantazopoulou SJ. Recovery of seismic resistance in corrosion-damaged reinforced concrete through FRP jacketing. *Int J Mater Product Technol* 2005;23(3/4):389–415.
- [30] Warner RF, Rangan B, Hall AS, Faulkes KA. Concrete structures. Melbourne: Longman Press; 1998.
- [31] Nowak AS, Szerszen MM, Szeliga EK, Szwed A, Podhorecki PJ. Reliability-based calibration for structural concrete. Report No. UNLCE 05-03, Department of Civil Engineering, University of Nebraska; 2005.
- [32] Otsuki N, Miyazato S, Diola NB, Suzuki H. Influence of bending crack and water–cement ratio on chloride-induced corrosion of main reinforcing bars and stirrups. *ACI Mater J* 2000;97(4):454–64.
- [33] Vu KAT. Corrosion-induced cracking and spatial time-dependent reliability analysis of reinforced concrete structures. PhD Thesis, The University of Newcastle, NSW, Australia; 2003.
- [34] Enright MP, Frangopol DM. Condition prediction of deteriorating concrete bridges. *J Struct Eng, ASCE* 1999;125(10):1118–25.
- [35] Ellingwood B, Galambos TV, MacGregor JG, Cornell CA. Development of a probability based load criterion for American National Standard A58. National Bureau of Standards Special Publication 577, US Government Printing Office, Washington, DC; 1980.
- [36] Ellingwood BR, Culver CG. Analysis of live loads in office buildings. *J Struct Div, ASCE* 1977;103(ST8):1551–60.
- [37] Chalk PL, Corotis RB. Probability models for design live loads. *J Struct Div, ASCE* 1980;106(ST10):2017–33.
- [38] Philpot TA, Rosowsky DV, Fridley KJ. Serviceability design in LRFD for wood. *J Struct Eng, ASCE* 1993;119(12):3649–67.
- [39] ANSI/ASCE 7-93. Minimum design loads for buildings and other structures. New York: ASCE; 1994.
- [40] Andrade C, Alonso C. Values of corrosion rates of steel in concrete to predict service life of concrete structures, application of accelerated corrosion tests to service life prediction of materials. In: Cragnolino G, Sridhar N, editors, ASTM STP 1194. Philadelphia: American Society for Testing and Materials; 1994. p. 282–95.
- [41] Dhir RK, Jones MR, McCarthy MJ. PFA concrete: chloride-induced reinforcement corrosion. *Mag Concrete Res* 1994;46(169):269–77.
- [42] BRITE/EURAM. The residual service life of reinforced concrete structures. Final Technical Report. Report No. BRUE-CT92-0591; 1995.
- [43] Roberts MB, Atkins C, Hogg V, Middleton C. A proposed empirical corrosion model for reinforced concrete. *Proc Instit Civil Eng Struct Build* 2000;140:1–11.